ISSN: 2688-8645

Analysis of the Spatial and Temporal Distribution Pattern of Carbon Emissions from Ships In Ports

Guoxin Liu [1], Jianwen Ma [2, 3]

[1] School of Shipping College, Shandong Jiaotong University, Weihai Shandong, 264200, China

[2] School of Intenational Business, Shandong Jiaotong University, Weihai Shandong, 264200, China

[3] School of Merchant Marine, shanghai Maritime University, Shanghai 201200, China

Abstract

Against the backdrop of the "Dual Carbon" goal proposed during the 14th Five-Year Plan period, China's infrastructure development is advancing toward green and low-carbon patterns, in which ship carbon emissions have become a major environmental issue. As an effective tool for recording ship activities, Automatic Identification System (AIS) data provides a reliable means to accurately quantify carbon emissions. Based on AIS data, this paper adopted a grid method combined with the STEAM model to estimate ship carbon emissions in a port area by zone, and introduced the Spearman correlation coefficient to analyze the spatio-temporal distribution of ship carbon emissions from four aspects: time, space, ship navigation status, and traffic flow factors. The results show that the total CO_2 emissions of Qingdao Port in September 2022 were estimated to be 47705.62 tons, with oil tankers accounting for 38.6% of total emissions. In terms of navigation status, carbon emissions from moored ships accounted for more than half of the total emissions in the studied waters of Qingdao Port. Temporally, different ship types exhibited consistent hourly variation patterns, with high-emission periods concentrated from 22:00 to 06:00. Spatially, the highest carbon emissions were mainly concentrated in Qianwan Port Area, main fairways, anchorages, and some terminal zones. Regarding traffic flow factors, carbon emissions showed moderate-to-high positive correlations with ship density for different vessel types, and low positive or no correlations with ship speed. This study thoroughly analyzes the carbon emission characteristics of ships in Qingdao Port waters. The proposed method can be further applied to ports and waterways, providing valuable references for understanding ship carbon emissions and formulating targeted mitigation measures, as well as theoretical support for port regulatory policies on ship carbon emissions.

Keywords

AIS Data; Carbon Emissions; Spatio-temporal Analysis; Navigation Status.

1. Introduction

CO_2 emissions from the shipping industry account for approximately 3% of global total emissions. Without effective intervention, global ship greenhouse gas emissions could increase by 150%–250% in 2050 compared with 2012, raising their share of global emissions significantly. As a major maritime country, China is home to seven of the world's top ten ports. As critical hubs connecting maritime and land transport, ports are major sources of carbon emissions in the shipping sector, with ship emissions in port waters accounting for 60% of total port emissions. Therefore, establishing a localized ship carbon emission inventory based on port ship data and analyzing its spatio-temporal evolution is essential to support sustainable management and carbon reduction policies for port vessels.

ISSN: 2688-8645

The Automatic Identification System (AIS), composed of shore-based facilities and on-board equipment, is a digital navigation aid system for ship–shore and ship–ship communication. AIS collects real-time traffic data and records static, dynamic, and navigation information of ships, serving as a key source of maritime traffic big data. Integrating AIS data with ship databases enables dynamic calculation of ship carbon emissions and has become a mainstream approach in relevant research. Current studies mainly focus on the accuracy and uncertainty of emission estimation and the compilation of ship emission inventories, with insufficient analysis of the spatio-temporal distribution of carbon emissions by different ship types in port waters. Limited understanding of emission behavioral characteristics makes refined and targeted control of ship carbon emissions difficult. To effectively control port carbon emissions and achieve green and low-carbon port development, it is necessary to investigate the spatio-temporal distribution of ship carbon emissions in port areas.

Ship carbon emission estimation methods are mainly divided into top-down and bottom-up approaches. The top-down method approximates emissions based on fuel consumption and CO_2 emission factors. However, it suffers from low accuracy, lacks spatial-temporal attributes, and cannot meet refined estimation requirements due to scattered ship locations and limited access to fuel consumption data. To address these limitations, researchers have developed the bottom-up method, a dynamic emission calculation approach based on AIS data, engine power, load factors, and corresponding emission factors. This method improves accuracy by classifying navigation statuses in detail and optimizing emission factor selection, making it the dominant method for ship emission estimation. Representing the bottom-up framework, the Ship Traffic Emission Assessment Model (STEAM) was proposed by Jalkanen et al. for estimating ship exhaust emissions in the Baltic Sea. Later, Jalkanen et al. extended the model to include PM and CO calculations, incorporated impacts of ship loading, fuel types, and emission reduction technologies, and developed STEAM2. The STEAM model has been widely used in global and regional ship emission studies, with continuous improvements in estimation accuracy.

Existing research on the spatio-temporal distribution of ship carbon emissions is mostly embedded in regional emission inventory analysis, with few targeted investigations on port waters. Internationally, Figenschau et al. collected ship traffic data and emissions of CO_2, NO_x, SO_2, PM, and black carbon along the Northern Sea Route (NSR) in 2013 and analyzed seasonal and spatial variations. Bojić et al. developed an adaptive analytical model, compiled a total emission inventory for Split Port (Croatia), and established the first high-resolution spatio-temporal profile of ship emissions in an urban port basin. In China, Zeng et al. estimated the 2018 ship emission inventory for Xiamen Port using the emission factor method based on ship activities and evaluated port eco-efficiency using environmental and social indicators. Meng et al. established a 2020 emission inventory for Dagang Port Area of Qingdao Port, analyzed the distribution of air pollutants and greenhouse gases, identified key emission sources, and assessed emission reduction potentials.

In summary, existing studies focus on ship carbon emission calculation and inventory compilation, with limited refined spatio-temporal analysis that fails to meet emission reduction requirements, especially in dense port waters. This study takes Qingdao Port as the research area, uses AIS data combined with grid partitioning and the STEAM model to estimate ship carbon emissions by zone, and applies the Spearman correlation coefficient to reveal spatio-temporal distribution and emission characteristics from temporal, spatial, and traffic flow perspectives. The results provide references for carbon emission mitigation and regional air quality management in port waters.

ISSN: 2688-8645

2. Data and Methodology

2.1. Data Source and Processing

Ship carbon emission accounting requires ship engine parameters including main engine power, auxiliary engine power, load factors, and CO_2 emission factors. AIS data provided by the HiFleet platform serves as the primary data source. Data preprocessing follows the AIS extraction method proposed by Liu et al., retaining key navigation information such as speed and course to ensure suitability for the developed model. Ship profile information including main engine power, auxiliary engine power, and maximum design speed is retrieved from the global shipping information service system using MMSI as the key. For ships with missing records, default parameters from the IMO Fourth GHG Study and Puget Sound Maritime Air Emissions Inventory are used to complete the dataset.

2.2. Grid Method

The grid method divides space into regular cells for management and analysis. This study uses ArcGIS Pro to partition the studied port waters into grids, enabling refined estimation and spatio-temporal analysis of ship carbon emissions at the grid level.

2.3. Zonal Estimation Model for Ship Carbon Emissions

This study employs the AIS-based Ship Traffic Emission Assessment Model (STEAM) to calculate ship carbon emissions, with the calculation framework shown in Figure .

According to the STEAM model, total emissions of a ship during a voyage are the sum of main engine, auxiliary engine, and boiler emissions:

According to the STEAM model, total emissions of a ship during a voyage are the sum of main engine, auxiliary engine, and boiler emissions:

$$E=Em+Ea+Eb \quad (1)$$

In Equation 1, E represents the total emissions, Em denotes the emissions from the main engine, Ea signifies the emissions from the auxiliary engine, and Eb stands for the emissions from the boiler.

The formula for calculating the emissions from the main engine is shown in Formula 2, where the main engine load factor is the cube of the ratio between the actual speed of the ship and its design speed [28], as shown in Formula 3

$$Em=Pm\times LFm\times T\times EFm\times FCF \quad (2)$$

$$LFm=(AS/MS)3 \quad (3)$$

Table 1. Host Emission Factor Table

engine type	construction time	NO_x	HC	CO	SO_2	PM_{10}	$PM_{2.5}$	DPM	CO_2	N_2O	CH_4
low speed	2000	18.1	0.6	1.4	10.5	1.5	1.2	1.5	620	0.031	0.012
	2000-2010	17.0	0.6	1.4	10.5	1.5	1.2	1.5	620	0.031	0.012
	2011-2015	14.4	0.6	1.4	10.5	1.5	1.2	1.5	620	0.031	0.012
mid-speed	2000	14.0	0.5	1.1	11.5	1.5	1.2	1.5	683	0.031	0.010
	2000-2010	13.0	0.5	1.1	11.5	1.5	1.2	1.5	683	0.031	0.010
	2011-2015	10.5	0.5	1.1	11.5	1.5	1.2	1.5	683	0.031	0.010

ISSN: 2688-8645

Table 2. Fuel Correction Coefficient Table

NO_x	VOC	CO	SO_2	PM_{10}	$PM_{2.5}$	DPM	CO_2	N_2O	CH_4
0.94	1.00	1.00	0.185	0.25	0.25	0.25	1.00	0.94	1.00

The calculation of emissions from marine auxiliary engines and boilers is related to the navigation status of the ship. Based on the navigation speed of ocean-going vessels, the navigation status of the ship is divided into five categories: cruising, low-speed cruising, port maneuvering, anchoring, and mooring [18], as shown in Table 3.

Table 3. Criteria for Determining the Navigation Status of Ships

Navigation status	Judgment conditions
mooring	speed ＜1 Section
Anchoring	1section＜speed＜3section
Minato Ward Mobile	3section＜speed＜8section
slow navigation	8section＜speed＜12section
cruise	Speed>12section

The calculation formulas for emissions from marine auxiliary engines and boiler emissions are shown in Equations 4 and 5:

$$Ea=Pa\times LFa\times T\times EFa\times FCF \quad (4)$$

$$Eb=Pb\times T\times EFb \quad (5)$$

In formula 45, Pa represents the rated power of the ship's auxiliary engine, Pb denotes the actual power of the boiler, LFa signifies the load factor of the auxiliary engine, T stands for the ship's navigation time, EFa and EFb respectively represent the emission factors of the auxiliary engine and boiler, and FCF stands for the fuel correction factor. The load factor of the auxiliary engine, emission factor of the auxiliary engine, and emission factor of the boiler are detailed in Table 4-6 [27][29].

Table 4. Load Coefficient of Auxiliary Machinery

Ship type	cruise	slow navigation	Minato Ward Mobile Unit	anchoring	mooring
passenger ship	0. 80	0. 80	0. 80	0. 64	0. 64
oil tanker	0.24	0.28	0.33	0.26	0.26
bulk carrier	0.17	0.27	0.45	0.22	0.22
container ship	0.13	0.25	0.48	0.19	0.19
Ro-ro ship	0.15	0.30	0.45	0.26	0.26
Other cargo ships	0.17	0.27	0.45	0.10	0.10
tugboat	0.17	0.27	0.45	0.22	0.22
Non-transport ship	0.17	0.27	0.45	0.22	0.22

Table 5. Auxiliary Machinery Emission Factor Table

Engine type	Construction time	NO_x	VOC	CO	SO_2	PM_{10}	$PM_{2.5}$	DPM	CO_2	N_2O	CH_4
medium speed	2000	14.7	0.5	1.1	12.3	1.0	0.8	1.0	683	0.031	0.008
	2000-2010	13.0	0.5	1.1	12.3	1.0	0.8	1.0	683	0.031	0.008
	2011-2015 year	10.5	0.5	1.1	12.3	1.0	0.8	1.0	683	0.031	0.008

ISSN: 2688-8645

Table 6. Boiler Emission Factor Table

NO_x	HC	CO	SO_2	PM_{10}	$PM_{2.5}$	DPM	CO_2	N_2O	CH_4
2.1	0.1	0.2	16.5	0.8	0.6	0.00	970	0.08	0.002

The emission calculation for each ship is carried out based on its reports from every two consecutive positions, typically at one-second intervals. In this article, the emission amount for the given voyage segment is recorded using the geographical coordinates of the subsequent reporting point. Based on the geographical coordinates of this point, its corresponding grid is determined, and the emission generated by this trajectory segment is then tallied within that grid. The calculation formula is as follows:

$$Q_j = \sum_{i=0}^{n} E_{ij} \tag{6}$$

In Equation 6, Qj represents the emission volume from ships in grid J, Eij denotes the emission volume from ship i in grid J, and N signifies all ships in grid J.

3. Case Analysis

3.1. Study Area

This study selects Qingdao Port waters as the research area. With high navigation density, diverse ship types, a long coastline in Jiaozhou Bay, and strong environmental pressure from ship emissions, Qingdao Port is suitable for verifying the proposed method. The study area spans 120.18°E–120.53°E and 35.91°N–36.07°N (Figure 2).

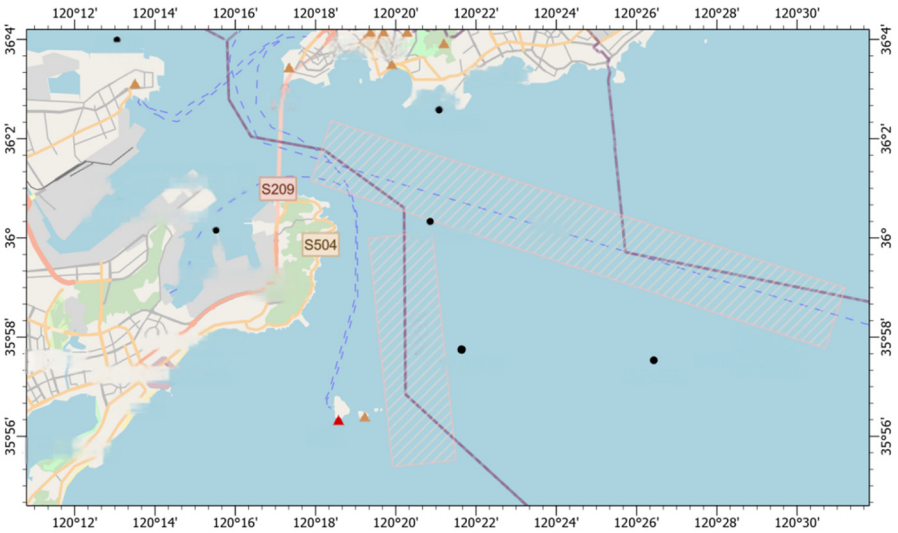

Figure 1. Study Waters

3.2. Estimation of Ship Carbon Emissions

This article employs the WGS 1984 Web Mercator coordinate system to grid the study area (120.18°E-120.53°E, 35.91°N-36.07°N), establishing 3432 grids of 500m×500m, and assigns an index number to each grid, thereby achieving high-precision measurement and calculation of ship emissions, as shown in Figure .

Taking into account the vessel traffic volume in Qingdao Port, we collected AIS data from September 2022 for research and analysis. The following eight categories of operating vessels were selected as the research subjects: container ships, other cargo ships, tankers, tugs, bulk carriers, passenger ships, roll-on/roll-off ships, and non-transport ships.

ISSN: 2688-8645

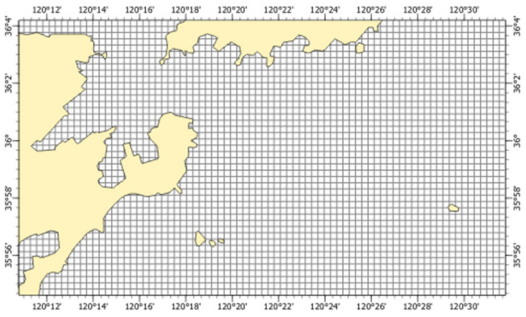

Figure 2. Grid map of the study water area

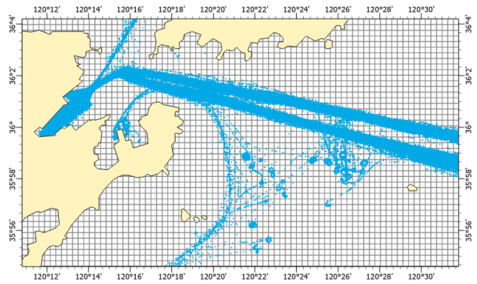

(a)Container ship

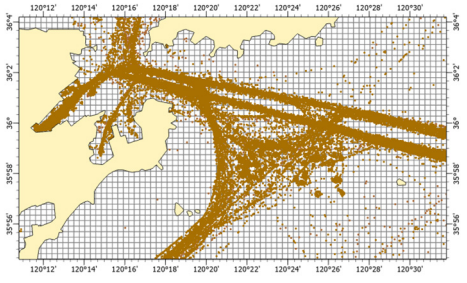

(b) Other cargo ships

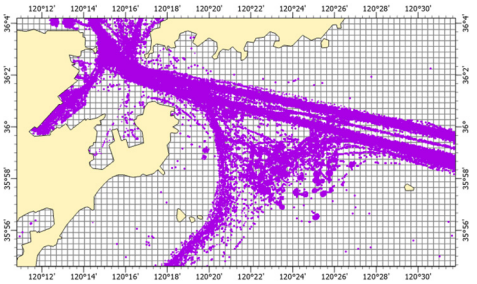

(c) Oil tanker

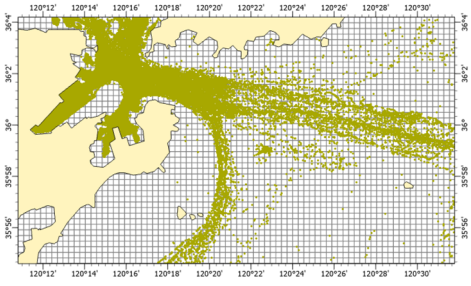

(d) Tugboat

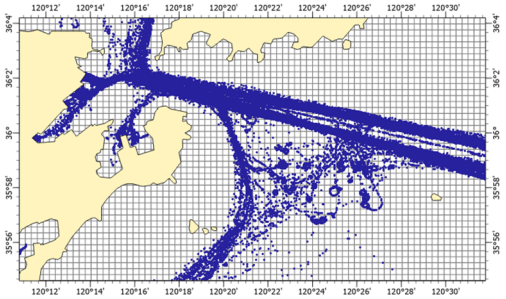

(e) Bulk carrier

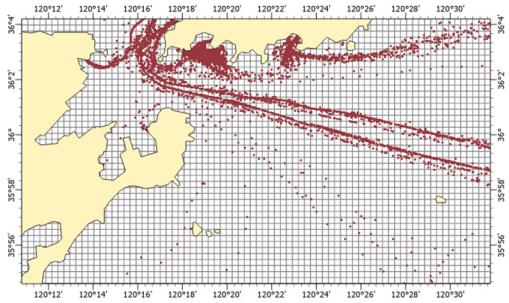

(f) Passenger ship

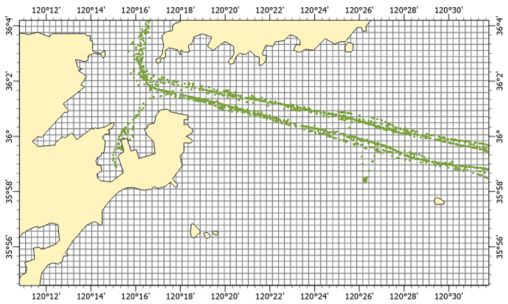

(g) Ro-ro ship

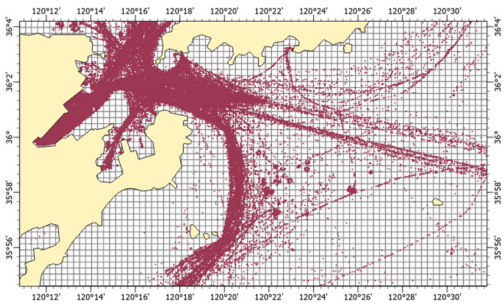

(h) Non-transport ship

Figure 3. Visualization of Ship Trajectory

ISSN: 2688-8645

Among them, passenger ships include high-speed passenger ships, ordinary passenger ships, and cruise ships; tankers include oil tankers, chemical tankers, and general liquid cargo ships; other cargo ships include dry cargo ships and general cargo ships; non-transport ships include engineering ships, service ships, and special-purpose ships. After processing with the aforementioned method, a total of 1,346 research vessels were obtained, with a total of 1,799,031 AIS data entries. The visualization effect of their trajectories is shown in Figure.

By comprehensively applying the aforementioned methods and utilizing the ship carbon emission zoning estimation model, it is possible to obtain the total carbon emission within the study scope of Qingdao Port, which is approximately 47,705.62 tons. The carbon emissions of various ship types are presented in Table 7;

Table 7. Carbon Emissions of Different Types of Ships

Ship Type	Number of ships	AIS data	Ship carbon emissions (t)
passenger ship	32	58889	5258.843
oil tanker	165	153324	18416.251
bulk carrier	172	149723	2551.843
container ship	519	410812	14910.140
Ro-ro ship	9	4167	195.063
Other cargo ships	252	233009	2752.440
tugboat	59	483781	2186.997
non-transport ship	138	305326	1434.043

To analyze the distribution of carbon emissions from different types of ships, this paper conducts a study on the carbon emission share of various ship types. The specific results are shown in Figure 5, where tankers have the highest carbon emissions, totaling 18,416.251 tons, accounting for 38.6% of the total carbon emissions from ships; followed by container ships, with a total of 14,910.14 tons, accounting for 31.3% of the total emissions; then passenger ships, other cargo ships, bulk carriers, tugs, and non-transport ships, with carbon emissions of 5,258.843 tons, 2,752.44 tons, 2,551.843 tons, 2,186.997 tons, and 1,434.043 tons, respectively, accounting for 11%, 5.8%, 5.3%, 4.6%, and 3% of the total emissions; ro-ro ships have the least emissions, totaling 195.063 tons, accounting for 0.4% of the total emissions.

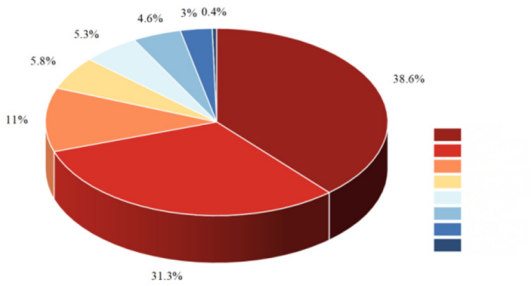

Figure 4. Sharing Rate of Ship Carbon Emissions in the Studied Waters

To gain a deeper understanding of the carbon emission levels of different types of ships, we next conducted a statistical analysis on the proportion of different types of ships. The results are shown in Figure 6, where container ships are the most numerous, accounting for 38.6% of the total. Comparing Figures 5 and 6, it can be seen that tankers and container ships account for 69.9% of the total emissions, showing a significant gap compared to other types of ships. The number of tankers accounts for only 12.3% of the total number of ships, but their emissions

ISSN: 2688-8645

are the highest, which is due to the high boiler load power when they are moored. Container ships are the most numerous, accounting for 28.6% of the total, and therefore have a large emission volume. The number and emission volume of passenger ships, other cargo ships, bulk carriers, tugs, and non-transport ships are basically similar. Due to the high proportion of high-speed passenger ships in Qingdao Port and the behavior of ships berthing and waiting for passengers, their number is relatively small but their carbon emissions are high. Ro-Ro ships have the lowest emissions and proportion of ships.

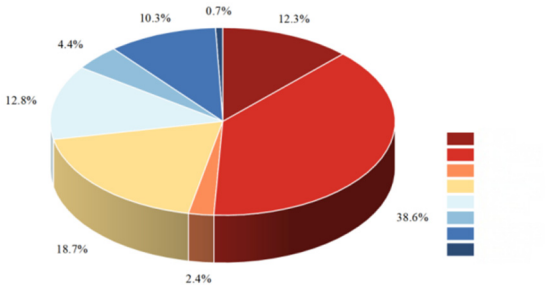

Figure 5. Proportion of the number of different types of ships

3.2.1. Navigation Status Analysis

Carbon emissions by navigation status are shown in Figure . Moored ships account for 75.6% of total emissions, followed by low-speed cruising (10.7%) and cruising (7.0%). Auxiliary engines and boilers operate at higher power during mooring, leading to dominant emissions. Reducing emissions during the mooring period is critical for port carbon mitigation.

To gain a more comprehensive understanding of the differences in carbon emissions during the operation of different types of ships, this article investigates the proportion of carbon emissions from different types of ships under various navigation conditions, as illustrated in Figure . Apart from tugs, other types of ships primarily operate in a moored state. Tugs are mainly engaged in low-speed navigation and port maneuvering; other types of ships spend more time in a moored state. Qingdao Port is one of the top ten ports in the world, with the Qianwan Port Area, Haixiwan Port Area, and Huangdao Port Area serving as important cargo terminal operation areas. Every day, a large number of ships berth at the port waiting for operations. For instance, tugs are primarily used to assist large ships in entering and exiting the port, as well as in ship maneuvering, berthing, and departing, leading to increased emissions during navigation. Meanwhile, other transport ships wait for passengers to board or cargo to be loaded and unloaded at the port, resulting in increased emissions during the moored state. These processes often require the boilers to be kept running to maintain ship functionality and comfort, thereby leading to increased emissions during the moored state.

3.3. Spatio-Temporal Distribution of Ship Carbon Emissions

3.3.1. Temporal Distribution

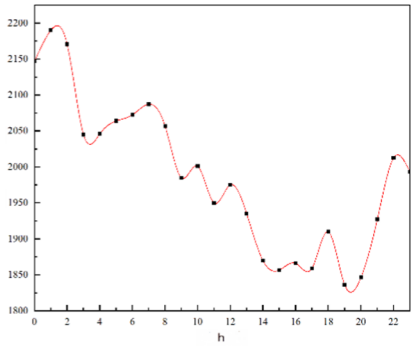

Figure 6. Hourly Variation of Ship Emissions at Qingdao Port

ISSN: 2688-8645

Hourly emission patterns (Figure 6) show consistent trends across ship types: high emissions from 22:00 to 06:00 and low emissions from 14:00 to 20:00. Nighttime mooring with boiler operation drives higher emissions.

3.3.2. Spatial Distribution

To investigate the distribution of carbon emissions from ships in the navigation area, this paper employs a zoned estimation model for ship carbon emissions combined with a grid visualization method, and the results are presented in Figure 10. As evident from Figure 10, within the study area, the maximum grid emission exceeds 605 tons, while the minimum is less than 0.00034 tons, indicating significant numerical fluctuations. Among these, there are a total of 1,050 grids with emissions greater than 1 ton, accounting for 40.71% of the total number of grids after excluding those located on land within the study watershed; there are a total of 15 grids with emissions greater than 605 tons, accounting for 0.58% of the total. Overall, the ship emissions in Qingdao Port are relatively high, and the carbon emission areas align with the functional zones of Qingdao Port, primarily concentrated in the port areas (Qianwan Port Area, Haixi Bay Port Area, Huangdao Port Area), the port entrance and exit areas, the navigation channels (main channel, fourth channel), the anchorage areas, and the docks (passenger docks).

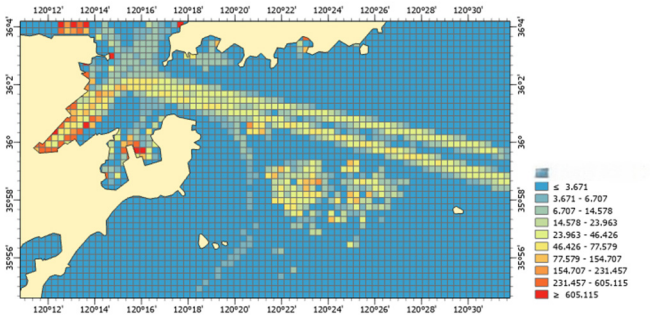

Figure 7. Spatial distribution map of ship carbon emissions

To further analyze the distribution of carbon emissions from different types of ships within the study area, the carbon emission calculation results for each type of ship in September 2022 were plotted into a 500m x 500m spatial distribution map of carbon emissions, as shown in Figure. From Figure 11, it can be observed that the carbon emission areas of container ships are mainly concentrated in the main channel and the port entrance and exit areas, with a small distribution in the dock and anchorage areas. This is because container ships have a high overall speed and a high load factor of the main engine, resulting in the highest carbon emissions in the main channel area. Other cargo ships, with their relatively high speeds and high load factors of the main engine, have a uniform distribution of carbon emissions in the main channel and anchorage areas, with a relatively higher concentration in the Qianwan port area. Bulk carriers have their carbon emissions concentrated in the channels and anchorage areas, which are less compared to other cargo ships. Oil tankers have a significant distribution of carbon emissions in the main channel, the fourth channel, the port area, and the anchorage area. This is due to the large volume, heavy weight, and high speed of oil tankers, which result in the highest emission factors of auxiliary engines and boilers during berthing and unloading, leading to high carbon emissions from oil tankers. Due to the particular nature of their work, tugboats mainly distribute their carbon emission areas in the port area, with a small distribution in the channels. Passenger ships have a significant distribution of carbon emissions in the docks and channels west of Taiping Bay. Due to their high speed, high density, and the behavior of berthing and waiting for passengers, the loads of auxiliary engines and boilers are high, resulting in increased carbon emissions from ships. Ro-Ro ships have their carbon emissions concentrated in the main channel and the Haixi Bay port area. Non-transport ships mainly distribute their carbon

ISSN: 2688-8645

emissions in the port area and the port entrance and exit areas, with less carbon emissions near the channels.

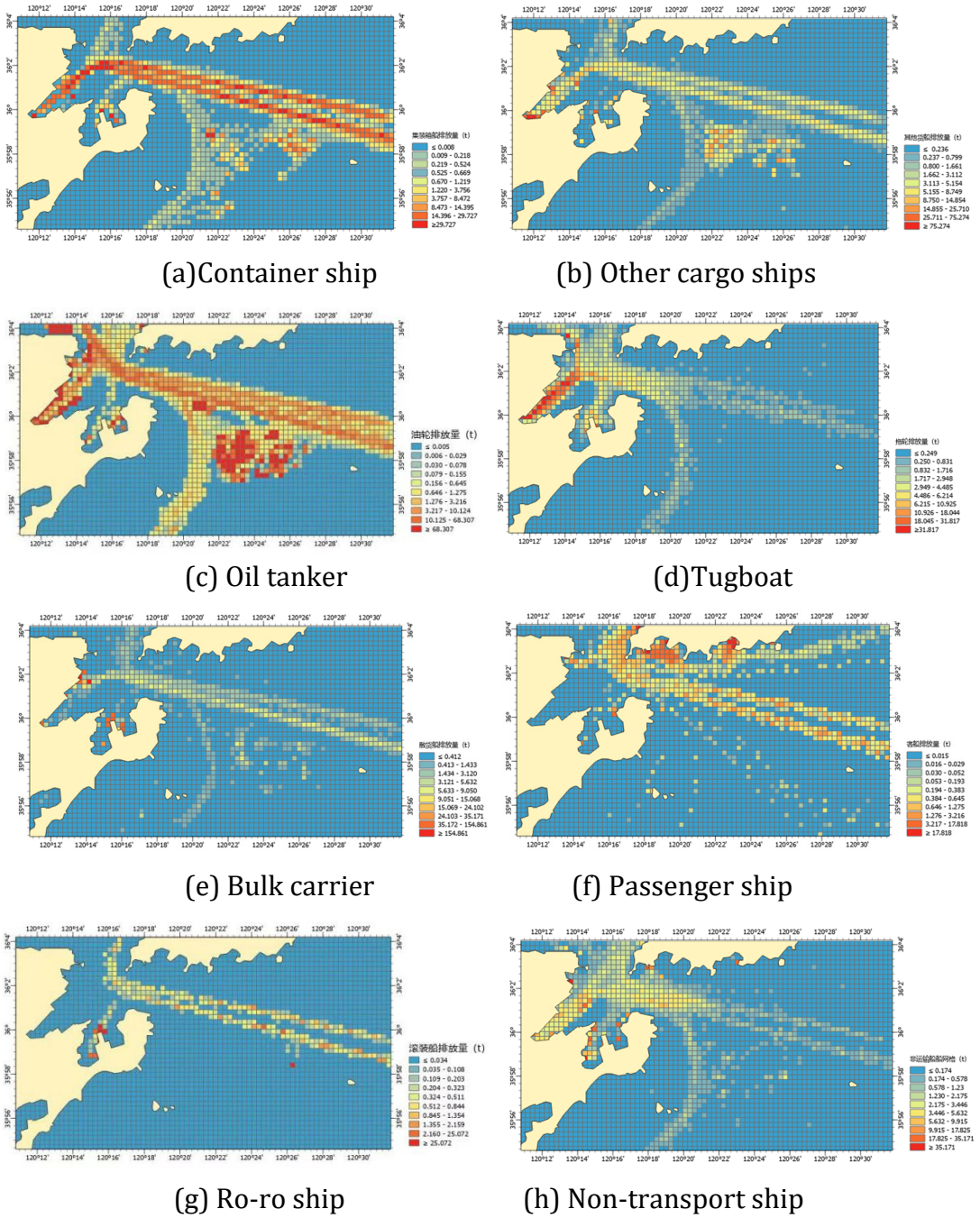

(a)Container ship (b) Other cargo ships

(c) Oil tanker (d)Tugboat

(e) Bulk carrier (f) Passenger ship

(g) Ro-ro ship (h) Non-transport ship

Figure 8. Spatial Distribution Map of Carbon Emissions from Different Types of Ships

3.3.3. Ship Attribute Analysis

To explore the correlation between different ship attributes and ship carbon emissions in port waters, each grid was taken as a unit to establish a one-to-one correspondence between ship density, average ship speed, and ship carbon emissions, resulting in a total of 1176 sets of data. Since the obtained data were all small sample sizes (sample size ≤ 5000), this paper conducted a Shapiro-Wilk normality test on the data and found that the sample data did not conform to a normal distribution. Therefore, the Spearman correlation coefficient was used for correlation analysis [30-31]. The formula for calculating the Spearman correlation coefficient is as follows:

ISSN: 2688-8645

$$\rho=1-\frac{6\sum_{i=1}^{n}d_i^2}{n(n^2-1)} \tag{7}$$

In the formula, ρ represents the Spearman correlation coefficient; n denotes the sample size; and di signifies the rank difference of the sample data.

Based on the distribution characteristics of the number of ships in Qingdao Port's navigation channels, this section utilizes the DBSCAN method to perform density clustering on operating ships, with a neighborhood radius set at 5, as shown in Figures 12 and 15. According to the distribution of ship trajectories, to explore the correlation between ship carbon emissions and ship speed, the average ship speed was calculated, and the calculation results are shown in Figures 13 and 16.

To further analyze the impact of the number of operating ships on carbon emission levels, the DBSCAN method was employed to conduct density clustering analysis on the study area of operating ships. This allowed us to obtain the spatial distribution of ship numbers and carbon emission levels in different density regions. The specific results are shown in Figure . The hotspot areas of operating ships studied are mainly concentrated in the Huangdao Port Area, Qianwan Port Area, Haixi Bay Port Area, Passenger Terminal Area, and the vicinity of Qianhai Anchorage Grounds 2 and 3.

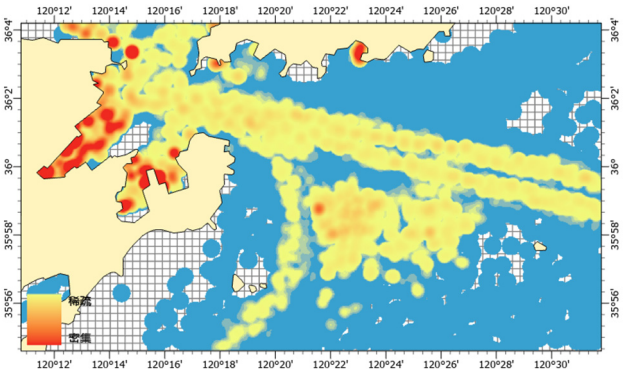

Figure 9. Distribution Map of Operating Vessel Density

To gain a deeper understanding of the differences in carbon emission levels during the navigation of operational ships, the DBSCAN method was employed to conduct cluster analysis on the trajectory speeds of operational ships. Ships were categorized into different clusters based on their varying movement speeds within the study area. The specific results are illustrated in Figure 13. There are significant differences in the distribution of ship trajectories and speeds across different regions. The operational ships studied exhibited higher overall speeds on the main channel, while their average speeds were lower in port areas, anchorages, and dock areas.

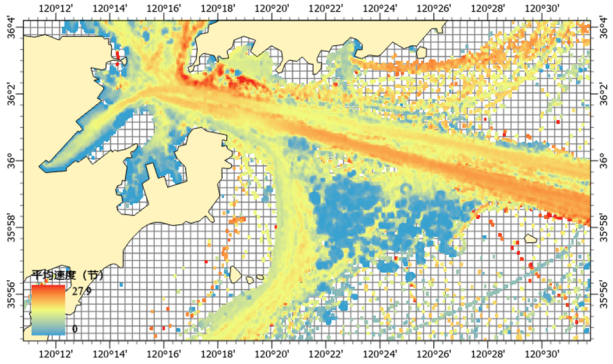

Figure 10. Distribution Diagram of Operating Vessels' Speeds

ISSN: 2688-8645

To further explore the distribution characteristics of carbon emissions in Qingdao Port, this section utilizes the Spearman correlation coefficient to analyze the correlation between ship density and average speed. The specific results are shown in Figure .

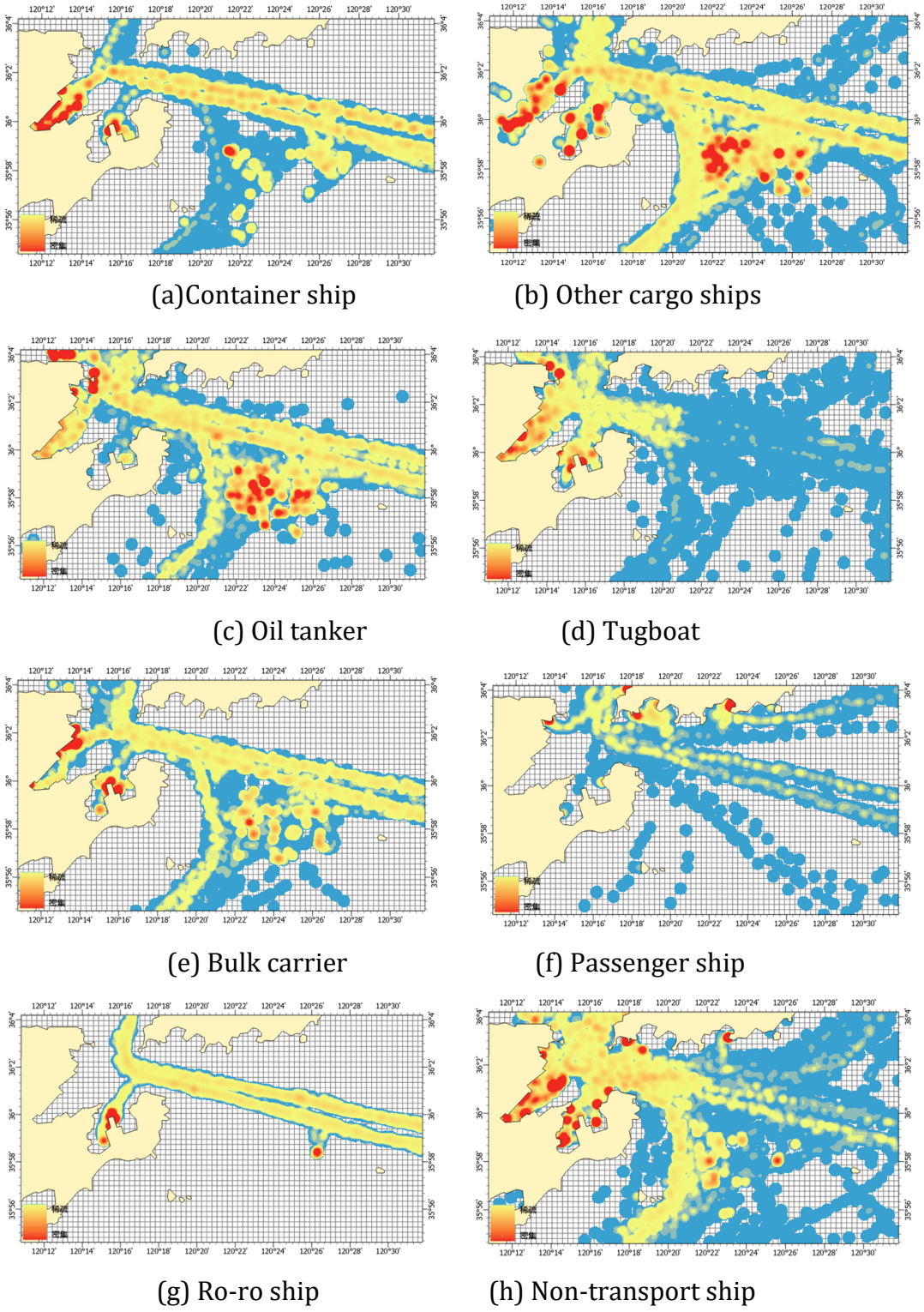

(a)Container ship (b) Other cargo ships

(c) Oil tanker (d) Tugboat

(e) Bulk carrier (f) Passenger ship

(g) Ro-ro ship (h) Non-transport ship

Figure 11. Heat map of density of different types of ships

As can be seen from Figure , there are significant differences in emissions, average speed, and ship density among operating ships at the 1% level, indicating a correlation relationship, which is a positive low-level correlation. The correlation coefficients between the average speed and

ISSN: 2688-8645

emissions, as well as ship density, for different types of ships are 0.099∗∗ and 0.93∗∗, respectively, both indicating a positive low-level correlation. The correlation coefficients between ship density and emissions, as well as average speed, for different types of ships are 0.93∗∗ and 0.059∗∗, respectively, indicating a positive high-level correlation between ship density and emissions, and a positive low-level correlation between ship density and average speed.

To better explore the distribution patterns of carbon emissions from different types of ships, we categorize ships by type and further analyze the density and speed distribution of each type.

(1) Ship density and carbon emissions

Using DBSCAN density clustering, we conducted density clustering on different types of ships, and the results are shown in Figure .

As shown in Figure , the areas with a high concentration of container ships are near the Qianwan Port Area, Haixi Bay Port Area, and Qianhai Anchorage No. 2; the areas with a high concentration of other cargo ships are near the Qianwan Port Area, Haixi Bay Port Area, and Qianhai Anchorage Nos. 2 and 3; the areas with a high concentration of oil tankers are near the Huangdao Port Area and Qianhai Anchorage Nos. 2 and 3; the areas with a high concentration of tugboats are near the Huangdao Port Area, Qianwan Port Area, and Haixi Bay Port Area; the areas with a high concentration of bulk carriers are near the Huangdao Port Area and Qianwan Port Area; the areas with a high concentration of passenger ships are in the passenger terminal area; the areas with a high concentration of roll-on/roll-off ships are in the Haixi Bay Port Area; and the areas with a high concentration of non-transport ships are in the Qianwan Port Area, Haixi Bay Port Area, and passenger terminal area. Using grids as units, the Spearman correlation coefficient was calculated for the ship emissions and ship density in each grid, and the results are shown in Table 8 below. Here, ∗∗ and ∗ represent significance levels of 1% and 5%, respectively; + and - represent positive and negative correlations, respectively; the correlation levels are divided into low correlation (0 to 0.5), moderate correlation (0.5 to 0.7), and high correlation (0.7 to 1). Using grids as units, the Spearman correlation coefficient was calculated for the ship density and carbon emissions in each grid, and the results are shown in Table 8 below.

Table 8. Correlation Coefficients of Different Types of Ship Density

Types of ships	container ship	Other cargo ships	oil tanker	tugboat	bulk carrier	passenger ship	Ro-ro ship	Non-transport ship
correlation coefficient	0.967**	0.915**	0.908**	0.860**	0.861**	0.779**	0.677**	0.863**

According to Table 8, there are significant differences in ship density and carbon emissions among different types of ships at the 1% level, indicating a correlation between the two, which is positive. Among them, the correlation coefficient between container ship density and carbon emissions is the highest, at 0.967, followed by other cargo ships, oil tankers, non-transport ships, bulk carriers, tugs, and passenger ships, with correlation coefficients of 0.915, 0.908, 0.863, 0.861, 0.860, and 0.779, respectively. The ship density and carbon emissions of the above types of ships are highly positively correlated; however, the correlation coefficient between ro-ro ship density and carbon emissions is 0.677, indicating only a moderate positive correlation between the two.

(2) Average ship speed and carbon emissions

Based on the distribution of ship trajectories, the average ship speed was calculated, and the calculation results are shown in Figure .

ISSN: 2688-8645

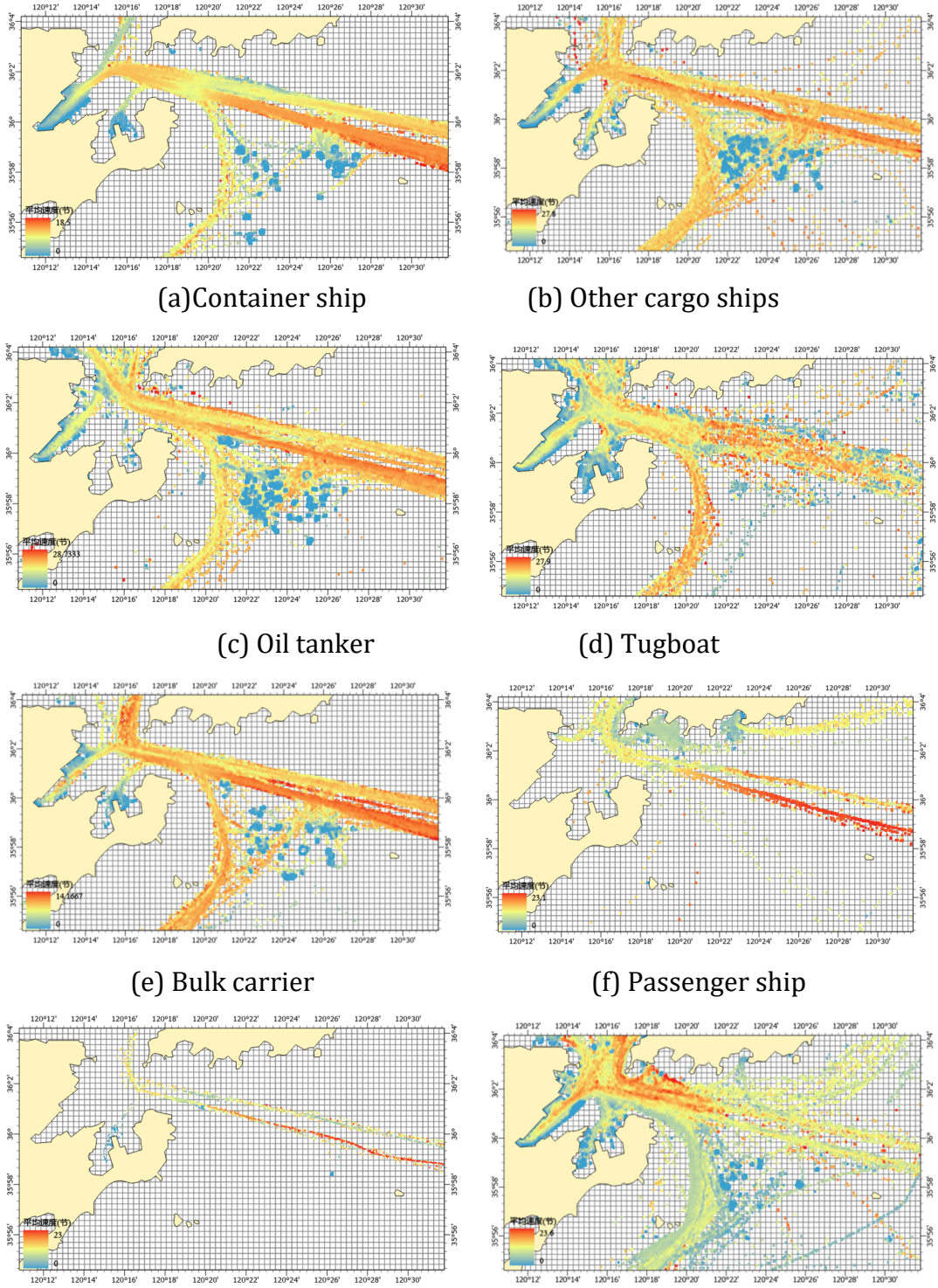

(a)Container ship (b) Other cargo ships

(c) Oil tanker (d) Tugboat

(e) Bulk carrier (f) Passenger ship

(g) Ro-ro ship (h) Non-transport ship

Figure 12. Heat map of average speeds of different types of ships

As shown in Figure , there are significant differences in ship trajectories and speed distributions among different types of ships. Container ships, other cargo ships, tankers, tugs, bulk carriers, passenger ships, and ro-ro ships have higher average speeds in the main channel, while non-transport ships have higher average speeds in the port entrance and exit areas. All types of ships have lower average speeds in the port area, anchorage, and dock area. Taking each grid as a unit, the Spearman correlation coefficient between the average speed of ships within each grid and carbon emissions is calculated, and the results are shown in Table 9 below.

ISSN: 2688-8645

Table 9. Correlation Coefficients of Average Speeds of Different Types of Ships

Types of ships	container ship	Other cargo ships	oil tanker	tugboat	bulk carrier	passenger ship	roll-on/roll-off ship	non-transport ship
correlation coefficient	0.159**	0.054*	0.081**	0.092**	0.198**	-0.015	0.204**	0.216**

According to Table 9, there is no significant correlation between the average speed and carbon emissions of passenger ships, indicating no correlation between the two; there is a significant difference in average speed and carbon emissions at the 5% level for other cargo ships, but the correlation coefficient is 0.054, indicating only a positive low-level correlation between the two; there is a significant difference in average speed and carbon emissions at the 1% level for non-transport ships, roll-on/roll-off ships, bulk carriers, container ships, tugs, and tankers, but the correlation coefficients are 0.216, 0.204, 0.198, 0.159, 0.092, and 0.081, respectively, indicating only a positive low-level correlation between the two.

4. Conclusion

As one of the fastest-developing coastal ports in China, Qingdao Port features multiple terminals and specialized cargo-handling facilities, with shipping vital to regional economy. Using a bottom-up power-based method, this study estimates total ship carbon emissions at 47705.62 tons in the study area. Oil tankers dominate (38.6%), followed by container ships, passenger ships, and other cargo ships; tugboats and non-transport ships contribute less. Mooring is the largest emission source, highlighting status-specific emission patterns.

Ship carbon emissions are jointly driven by temporal, spatial, and traffic flow factors. Temporally, hourly emissions show a “low–high–low” pattern, peaking from 22:00 to 06:00 and bottoming from 14:00 to 20:00. Spatially, high-emission grids cluster in port areas and main fairways, including port entrances, fairways, terminals, and anchorages. In terms of traffic flow, emissions show low positive correlations with average speed and high positive correlations with ship density; average speed is weakly positively correlated with density and emissions.

Key mitigation measures include: optimizing berth allocation to reduce waiting and boiler operation; installing shore power systems to cut mooring emissions; using big data and AI to predict and optimize ship flow, reducing congestion during peak periods. The proposed method yields comprehensive indicators of ship carbon emissions at various spatio-temporal scales, clarifies traffic flow impacts on emissions, and provides scientific data support for port environmental management policy-making.

Acknowledgments

Natural Science Foundation.

References

[1] Huang, Liang, et al. "Estimation and spatio-temporal analysis of ship exhaust emission in a port area." Ocean Engineering 140 (2017): 401-411.

[2] IMO's Fourth Greenhouse Gas Study Report.

[3] IEC Technical Committee 80. Maritime Navigation and Radiocommunication Equipment and Systems. 2012.

[4] Huang, Liang, et al. "Dynamic calculation of ship exhaust emissions based on real-time AIS data." Transportation Research Part D: Transport and Environment 80 (2020): 102277.

[5] Chen Weijie, Song Bingliang, Zhang Jieshu. Carbon Emissions from Container Ports in China's Coastal Areas Based on AIS Data [J]. China Environmental Science, 2022, 42(07): 3403-3411. DOI: 10.19674/j.cnki.issn1000-6923.20220322.003.

[6] Gan, Langxiong, et al. "Ship exhaust emission estimation and analysis using Automatic Identification System data: The west area of Shenzhen port, China, as a case study." Ocean & Coastal Management 226 (2022): 106245.

[7] Shu, Yaqing, et al. "Evaluation of ship emission intensity and the inaccuracy of exhaust emission estimation model." Ocean Engineering 287 (2023): 115723.

[8] Huang, Hongxun, et al. "Inland ship emission inventory and its impact on air quality over the middle Yangtze River, China." Science of The Total Environment 843 (2022): 156770.

[9] Zhou, Chunhui, et al. "Identification and analysis of ship carbon emission hotspots based on data field theory: A case study in Wuhan Port." Ocean & Coastal Management 235 (2023): 106479.

[10] Eggleston, H. S., et al. "2006 IPCC guidelines for national greenhouse gas inventories." (2006).

[11] Miola A, Ciuffo B. Estimating air emissions from ships: Meta-analysis of modelling approaches and available data sources[J]. Atmospheric environment, 2011, 45(13): 2242-2251.

[12] Tan Jianwei, Song Yanan, Ge Yunshan, et al. Emission Inventory of Dalian Sea Area from Ocean-Going Vessels [J]. Environmental Science Research, 2014, 27(12): 1426-1431.

[13] Jalkanen J P, Brink A, Kalli J, et al. A modelling system for the exhaust emissions of marine traffic and its application in the Baltic Sea area[J]. Atmospheric Chemistry and Physics, 2009, 9(23): 9209-9223.

[14] Jalkanen, J-P., et al. "Extension of an assessment model of ship traffic exhaust emissions for particulate matter and carbon monoxide." Atmospheric Chemistry and Physics 12.5 (2012): 2641-2659.

[15] Johansson, Lasse, Jukka-Pekka Jalkanen, and Jaakko Kukkonen. "Global assessment of ship** emissions in 2015 on a high spatial and temporal resolution." Atmospheric Environment 167 (2017): 403-415.

[16] Yu Hongchu, Fang Qinglong, Fang Zhixiang, et al. Spatiotemporal distribution pattern of carbon emissions driven by ship dynamics [J]. China Environmental Science, 2024, 44(03): 1769-1776. DOI: 10.19674/j.cnki.issn1000-6923.2024.0078.

[17] Wan, Zheng, et al. "Ship** emission inventories in China's Bohai Bay, Yangtze River delta, and Pearl River delta in 2018." Marine Pollution Bulletin 151 (2020): 110882.

[18] Weng, J., Shi, K., Gan, X., Li, G., & Huang, Z. (2020). Ship emission estimation with high spatial-temporal resolution in the Yangtze River estuary using AIS data. Journal of Cleaner Production, 248, 119297.

[19] Woo, Donghan, and Namkyun Im. "Spatial analysis of the ship gas emission inventory in the port of busan using bottom-up approach based on AIS data." Journal of Marine Science and Engineering 9.12 (2021): 1457.

[20] Gao, X., Dai, W., & Yu, Q. (2024). Analysis of emission characteristics associated with vessel activities states in port waters. Marine Pollution Bulletin, 202, 116329.

[21] Figenschau, Nikolai, and **mei Lu. "Seasonal and Spatial Variability of Atmospheric Emissions from Ship** along the Northern Sea Route." Sustainability 14.3 (2022): 1359.

[22] Bojić, Filip, Anita Gudelj, and Rino Bošnjak. "An Analytical Model for Estimating Ship-Related Emissions in Port Areas." Journal of Marine Science and Engineering 11.12 (2023): 2377.

[23] Zeng Fantao, Lv Jing. Vessel Emission Inventory and Port Ecological Efficiency Evaluation of Xiamen Port [J]. China Environmental Science, 2020, 40(05): 2304-2311. DOI: 10.19674/j.cnki.issn1000-6923.2020.0264.

[24] Fan Yongji, Chen Xuan, Xie Hua, et al. Study on the emission inventory and characteristics of atmospheric pollutants from ships in Guangxi's inland rivers and coastal areas [J]. Journal of Environmental Engineering Technology, 2023, 13(06): 2072-2080.

[25] https://www.hifleet.com/.

ISSN: 2688-8645

[26] LIU Chang, ZHANG Shi-ze, LI Bei-ying, et al.Typical Ship Trajectory Extraction Method Considering Ground Speed and Headin[J].Journal of Transportation Systems Engineering and Information Technology,2022,22(06):114-123.

[27] Puget Soud Maritime Air Forum. Puget Sound Maritime Air Emissions lnventory.2012.

[28] Goldsworthy L, Goldsworthy B. Modelling of ship engine exhaust emissions in ports and extensive coastal waters based on terrestrial AIS data–An Australian case study[J]. Environmental Modelling & Software, 2015, 63: 45-60.

[29] Liu Yue, Chen Junfeng, Tian Yujun, et al. Characteristics of Air Pollutant Emissions from Ships in the Bohai Economic Zone [J]. Environmental Science Research, 2021, 34(03): 523-530. DOI: 10.13198/j.issn.1001-6929.2020.05.08.

[30] Schober P, Boer C, Schwarte L A. Correlation coefficients: appropriate use and interpretation[J]. Anesthesia & analgesia, 2018, 126(5): 1763-1768.

[31] Xu, Qianwen Ariel, and Victor Chang. "Co-authorship network and the correlation with academic performance." Internet of Things 12 (2020): 100307.